Desalination and Water Treatment
www.deswater.com
doi: 10.1080/19443994.2014.974215

56 (2015) 3519–3529
December

Taylor & Francis
Taylor & Francis Group

Evolution of electrolyte mixtures rejection behaviour using nanofiltration membranes under spiral wound and flat-sheet configurations

Mònica Reig[a,*], Neus Pagès[a], Edxon Licon[a], César Valderrama[a], Oriol Gibert[a,b], Andriy Yaroshchuk[a,c], José Luis Cortina[a,b]

[a]*Chemical Engineering Department, Universitat Politècnica de Catalunya, UPC-Barcelona TECH, Avd. Diagonal 647, 08028 Barcelona, Spain, Tel. +34 934016997; emails: monica.reig@upc.edu (M. Reig), neus.pages@upc.edu (N. Pagès), edxon.eduardo.licon@upc.edu (E. Licon), Tel. +34 934015877; email: cesar.alberto.valderrama@upc.edu (C. Valderrama), Tel. +34 934011818; email: oriol.gibert@upc.edu (O. Gibert), Tel. +34 934054443; email: andriy.yaroshchuk@upc.edu (A. Yaroshchuk), Tel. +34 934016570; email: jose.luis.cortina@upc.edu (J.L. Cortina)*
[b]*CETAQUA Carretera d'Esplugues, 75, 08940 Cornellà de Llobregat, Spain*
[c]*Catalan Institute for Research and Advanced Studies (ICREA), Barcelona, Spain*

Received 15 July 2014; Accepted 2 October 2014

ABSTRACT

Nanofiltration (NF) membranes can be used in different configurations. The aim of this work was to determine the reliability of the data obtained using flat-sheet (FS) laboratory-scale configuration when NF membranes are implemented at industrial scale level using spiral wound (SW) configuration. Ion rejections in salt mixtures with the two configurations types were analysed, modelled, evaluated and compared. In both cases of the study, the operation was carried out in cross-flow mode and with recirculation of permeate and concentrate streams into the feed tank. Different feed synthetic salt solutions were used based on a dominant and a trace salt. In both cases, the operating temperature was kept constant (21.5 ± 2.5°C), and the trans-membrane pressure range varied from the osmotic pressure to 20 bar. The same NF membrane was used for both configurations: NF270 (Dow Chemical). The solution–diffusion–electromigration–film model was employed to describe the experimental results. Comparing both membrane configurations, the trans-membrane flux obtained with the FS configuration was higher than that observed with the SW configuration under the same operating conditions. In general, it is proved that ion rejection curves for both membrane configurations were fairly similar. Moreover, the membrane permeances with respect to each ion in both configurations were quantitatively similar.

Keywords: Nanofiltration; Flat-sheet membrane; Spiral wound membrane; Ion rejection; Salt mixtures

*Corresponding author.

Presented at the IX Ibero-American Congress on Membrane Science and Technology (CITEM 2014), 25–28 May 2014, Santander, Spain

1. Introduction

Desalination plants are used to obtain potable water for human consumption. The concentration limits allowed for human consumption depend on the area, the health risk connected with these elements and the available technologies that each zone has to eliminate them [1].

Membrane technologies have become an important part of the separation processes during the last decades. Their applications have increased significantly in the water industry compared to other water treatment technologies. In particular, reverse osmosis (RO) and nanofiltration (NF) are broadly used for potable water treatment [2].

NF membranes have good rejections to divalent ions (up to 99%), but moderate rejection to monovalent ones in the difference of 20–70%. This property is an intermediate between RO membranes with a salt rejection of more than 95% and UF membranes with a salt rejection of less than 10% [3].

Compared to RO, NF offers some advantages, such as low operational pressure, high flux, high retention of multivalent ions, relatively low investment and low operation and maintenance costs. NF is signally useful for the potable water production, since using this technique, the remineralisation process of the obtained water during the process is reduced [4,5].

The module is the main part of any membrane plant. For this reason, some important aspects have to be taken into consideration for its design, such as packing density, cost-effective manufacture, easy access for cleaning and cost-effective membrane replacement. Based on the above, the modules can be distinguished into different major types: tubular module, hollow fibre module, plate and frame systems (flat-sheet modules (FS)) and spiral wound modules (SW) [6].

In FS configuration, the feed solution is pumped over one side of the membrane. Then, the filtration process is carried out in cross-flow mode. Due to a pressure gradient, part of the solution goes through the membrane (permeate stream). Packing densities of about 100–400 m^2/m^3 are achieved. FS membrane configuration is commonly used only at laboratory scale due to its size and low productivity. Although there are some FS modules at the industrial scale, it is uncomfortable to operate with them due to bearing a lot of layers and the high space requirements. The advantage of working at laboratory scale with any kind of membrane configuration is the low installation cost [7].

Essentially, in SW modules, two or more membrane pockets are wound around a centrally located permeate-collecting tube with a special mesh used as spacer. The membrane pocket consists of two membrane sheets with a highly porous material in between, which are glued together along three edges. The fourth edge of the pocket is connected to the collecting tube. Several such pockets are SW around the perforated permeate tube with a feed-side spacer placed between the pockets. Usually, several such membrane elements are arranged in one pressure vessel [6]. The feed-side flow is strictly axial, while the permeate flows through the porous support inside the pocket and along the spiral pathway to the collecting tube [8]. SW modules are characterized by high packing density (>900 m^2/m^3). This module is simple and is also resistant to fouling at higher pressures. Most of the commercially available NF membranes are made in SW configuration [9].

Recently, Ribera et al. [10] make a comparison of both membrane configurations working at constant trans-membrane pressure (TMP) and constant trans-membrane flux (Jv). They concluded that the experimentation at the laboratory scale plant can be useful to design a full-scale plant.

In this study, a comparison of both membrane configurations was carried out by changing both the TMP and the Jv. A rejection curve was obtained for each ion and each membrane configuration. Different synthetic mixtures based on a dominant salt combined with a trace salt were used as feed solution in each experiment. The solution–diffusion–electromigration–film model (SDEFM) was used to describe the experimental data. This model considers that the ion transport through the membrane occurs via solution–diffusion and electric migration phenomena, and also it takes into account the concentration polarization layer. The SDEFM was described by Yaroshchuk et al. [11]. By means of this model, it is possible to calculate the membrane permeability with respect to each ion, defined as the easiness of the ions to cross the membrane [12].

To sum up, FS configuration is usually used at laboratory-scale test membrane to evaluate the rejection of ions of interest by NF process under given conditions while at industrial scale SW membrane configuration are used, due to the need for a larger active membrane area and space optimization. The aim of this study was to determine the reliability of the data obtained using FS laboratory-scale configurations when they are implemented at industrial scale level using SW configurations.

2. Materials and methods

2.1. Experimental description and operation

Two experimental set-ups were used with FS and SW configurations in order to determine the influence of the membrane configuration on the ion rejection.

NF membranes used were NF270 (Dow Chemical Company, Midland, TX) with an effective membrane area of 0.014 m^2 for the FS configuration and 2.6 m^2 for the SW configuration.

Both membranes were composed of a semiaromatic piperazine-based polyamide layer on top of a polysulphone microporous support reinforced with nonwoven polyester [13]. The main characteristics of these membranes and operation limits of both pilot plants described by the manufacturer can be found in Table 1.

Fig. 1 shows schematic experimental set-ups for both membrane configurations.

The experimental procedure in both pilot plants was nearly the same. The feed solution (25 L for the FS configuration and 100 L for the SW one) was driven by a pump to the module where the membrane was located. Two streams were obtained: permeate and concentrate. Both streams were recirculated into the feed tank, so the feed concentration was kept approximately constant. Multiple parameter sensors were installed to monitor the process: pressure meters before and after the membrane, conductivity sensors, temperature sensors and flow meters in both permeate and concentrate stream. Adjustment of TMP was achieved through a needle valve settled in the concentrate stream. The TMP varied from the osmotic pressure to 20 bar, the permeate flow ranged between 1 and 3 L/min, and the temperature was kept constant (21.5 ± 2.5°C) A cartridge filter was used to protect the pump and also the membrane from fouling by erosion products.

Table 1
NF270 characteristics and operation limits of the pilot plants

Membrane type	Polyamide thin-film composite
Maximum operating temperature	45°C
Maximum operating pressure	41 bar
Maximum feed flow rate	1.4 m^3/h
Maximum pressure drop	1.0 bar
pH range, continuous operation	2–11
pH range, short-term cleaning (30 min)	1–12
Maximum feed silt density index	SDI 5
Free chlorine tolerance	<0.1 ppm

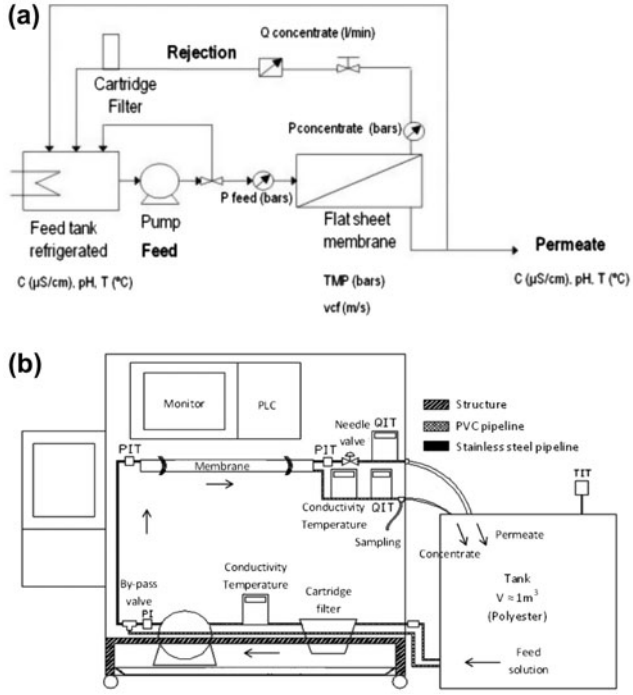

Fig. 1. Experimental set-up for the (a) FS and (b) SW membrane configurations.

To ensure that the comparison of the performances of both configurations was as objective and reliable as possible, the same feed solutions and operating conditions were used. These are summarized in Table 2.

Different synthetic aqueous solutions were used as feed solution for the experiments. All of them were based on a dominant salt (NaCl, $MgSO_4$, Na_2SO_4, and $MgCl_2$) mixed with trace ions (Na^+, Cl^-, Mg^{2+}, SO_4^{2-}, Br^-, NO_3^-, I^-, NH_4^+, and K^+). The ions studied are of great interest in brackish water purification, due to their large quantity (Na^+, Cl^-, Mg^{2+}, and SO_4^{2-}), they are precursors of trihalomethanes (Br^-, I^-) or they are characteristic ions present in rivers due to the influence of agriculture and industrial discharges (NO_3^-, K^+, and NH_4^+). The dominant salt concentration was always maintained at 0.1 mol/L, whereas the trace salt molar concentration was varied between 2 and 0.5% of dominant salt concentration depending on its solubility. All reagents used were of analysis quality (PA-ACS-ISO reagent, PANREAC).

Prior to any experiment, de-ionized water was pumped through the membrane modules at the maximum TMP during at least one hour and a half. Immediately after, this procedure was repeated with feed solution in order to ensure that the membrane density was kept constant during the whole experiment.

Table 2
Experimental design carried out in both configurations with electrolytes mixtures

		Feed concentration			
Dominant salt	Trace salt	Dominant salt (mol/L)	Trace salt (mol/L)	Trans-membrane pressure (bar)	Nanofiltration membrane
NaCl	$MgSO_4$	0.1	0.002	4.5–20	NF 270 (Dow Chemical)
	NaI	0.1	0.002	4.5–20	
	NaBr	0.1	0.002	4.5–20	
	$NaNO_3$	0.1	0.002	4.5–20	
	NH_4Cl	0.1	0.002	4.5–20	
	KCl	0.1	0.002	4.5–20	
$MgSO_4$	NaI	0.1	0.0005	4.5–20	
	NaBr	0.1	0.0005	4.5–20	
	$NaNO_3$	0.1	0.0005	4.5–20	
	NH_4Cl	0.1	0.0005	4.5–20	
Na_2SO_4	KCl	0.1	0.0005	7–20	
$MgCl_2$	NaI	0.1	0.0005	7–20	
	NaBr	0.1	0.0005	7–20	
	$NaNO_3$	0.1	0.0005	7–20	
	NH_4Cl	0.1	0.0005	7–20	
	KCl	0.1	0.0005	7–20	

After the pressurization procedure, the membrane was prepared to start the experiment with the feed salt solution. Then, a sample of the initial solution was taken. In each experiment, the temperature was kept constant, and the TMP was gradually increased by steps of 2 bars from the osmotic pressure to 20 bars. At each TMP increment, a permeate sample was collected once and its conductivity remained constant. Finally, one sample was collected from the feeding solution to corroborate that its composition was constant over the experiment.

2.2. Analytical methodologies and chemical analysis

During the experiments, solution rejections at each TMP were calculated with the online conductivity values. After that, the concentration of each ion in the samples was determined with an ionic chromatograph (Dionex ICS-1000). The cation and anion analyses were performed by two different analytical columns, IONPAC® CS16 and IONPAC® AS23 (Dionex), respectively.

2.3. Calculations of ion rejections

The results are presented in this study as ion rejection vs. Jv for both membrane configurations. Jv (m/s) was calculated for each sample, and it is defined as:

$$Jv = \frac{V}{tp \cdot A_{ef}} = \frac{m/\sigma}{tp \cdot A_{ef}} \quad (1)$$

where tp is the time of sample collection (s), V is the permeate volume collected during tp (m^3), A_{ef} is the effective membrane area (A_{ef} (FS) = 0.014 m^2; A_{ef} (SW) = 2.6 m^2), m is the liquid collected weight (kg), and σ is the density at 25°C (σ = 997.1 kg/m^3).

Experimental rejections (R) for different Jv were calculated with the ion concentrations obtained by chromatography.

$$R = \frac{C_F - C_P}{C_F} \quad (2)$$

where C_F is the ion concentration in the feed solution and C_P is the ion concentration in the permeate solution.

Next, dominant salt and trace ions rejections were calculated with the SDEFM by fitting the experimental data. In the cases where one of the trace ions is the same as one of the dominant ions, it is considered that its concentration is too low and only the dominant salt and the other trace ion rejections were calculated and fitted by the SDEFM.

2.4. Modelling experimental data

SDEFM was used to describe the ion rejection by the NF process, which was previously detailed in other publications [11,14]. The main assumption of the model is that the solute transport occurs via diffusion and electromigration, making the convection term negligible. The basic equation of the SDEFM (Eq. (3)) represents the ions flux in terms of concentration gradients and electric fields. It has been demonstrated previously that ions transfer in the NF membrane is controlled by the electric field, which appears due to the differences between the membrane permeabilities with respect to each dominant salt ion.

$$J_i = -D_i\left(\frac{dc_i}{dx} + z_i c_i \frac{d\varphi}{dx}\right) \quad (3)$$

where J_i is the trans-membrane flux of the solute i (mol/m^2s), D_i is the diffusion coefficient of the solute i (m^2/s), c_i is the concentration of solute i (mol/m^3), x is the trans-membrane coordinate (m), z_i is the charge of the solute i, and φ is the electrostatic potential [11].

The dominant salt ions control the electric field that arises in the NF membrane. The ion with higher membrane permeability with respect to it will be able to pass easily through the membrane, and an electric field will arise since the permeate side of the membrane will have opposite charge than the feed side [15]. For this reason, the dominant salt rejection was modelled in a first term for each solution.

SDEFM makes possible to calculate the observable rejection of the dominant salt and also the membrane and concentration polarization layer permeabilities. After that, the dominant salt intrinsic rejection and its concentration on the membrane surface are determined.

Subsequently, concentrations of the traces at the membrane surface and the intrinsic rejections of them are also calculated using the contribution of the concentration polarization layer.

In the particular case of a mixture of a single dominant salt and trace ions, it is possible to represent the reciprocal intrinsic transmission of a trace (f_t) as a function of the reciprocal intrinsic transmission of the dominant salt (f_s) as described in Eq. (4).

$$f_t = (f_s)^b + K\left(\frac{f_s - (f_s)^b}{1-b}\right) \quad (4)$$

where $f_s = \left(\frac{1}{1-R_s^{int}}\right)$, $f_t = \left(\frac{1}{1-R_t^{int}}\right)$, ${R_s}^{int}$ is the intrinsic rejection of the dominant salt, and ${R_t}^{int}$ is the intrinsic rejection of the trace ion.

From Eq. (4), it can be seen that experimental results can be fitted using only two parameters: $b \equiv \frac{Z_t(P_+ - P_-)}{Z_+P_+ - Z_-P_-}$, and $K \equiv \frac{P_s}{P_t}$, where Z_t is the charge of the trace ion, $Z_\pm$ is the charge to single ions of the dominant salt and P_s is the membrane permeability to the dominant salt.

Finally, the membrane permeability to single ions of the dominant salt ($P_\pm$) and to trace ions (P_t) are estimated using Eqs. (5) and (6), respectively [14].

$$P_\pm = \frac{P_s}{1 - \left(\frac{Z_\pm}{Z_t}\right)b} \quad (5)$$

$$P_t = \frac{P_s}{K} \quad (6)$$

To sum up, the SDEFM is able to predict the membrane permeability to the ions by estimating the parameters b and K when Eq. (4) is fitted to the experimental rejection curves in terms of Jv for each ion present in the solution.

3. Results and discussion

3.1. NaCl dominant

Fig. 2 shows the experimental rejections of NaCl (used as dominant salt) and Mg^{2+} and SO_4^{2-} (Fig. 2(a)) and NO_3^- (Fig. 2(b)) as traces for both FS and the SW configurations along different Jv and also the predicted rejections by the SDEFM.

The dominant salt and trace ion rejections are shown in Fig. 2. Generally, ionic species rejection using NF membranes describes an increasing curve as TMP, and consequently, Jv increases until a maximum rejection value where the rejection remains constant although varying the TMP. Fig. 2 shows that rejection trends under both configurations were similar.

In both cases, NaCl exhibited a moderate stable rejection at around 50%. The dominant salt rejection is independent of the trace salt (with divalent ions $MgSO_4$ or monovalent $NaNO_3$). It is known that NF membranes reject divalent ions better than single charge ones and that trace rejection depends only on the dominant salt rejection. The concentration of the trace is too low to modify the conditions in the membrane, thus, the use of a divalent (SO_4^{2-}) or monovalent ion (NO_3^-) as part of a trace salt does not represent a substantial effect on the NaCl rejection obtained for both experiments.

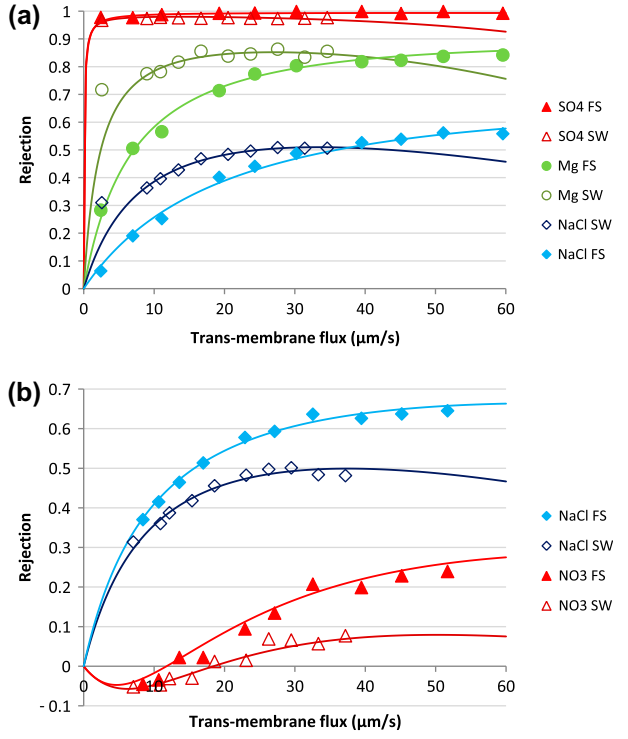

Fig. 2. Comparison between rejections experimentally obtained and rejections predicted with the SDEFM using a FS and a SW membrane configuration. (a) NaCl dominant salt and $MgSO_4$ as trace and (b) NaCl dominant salt and $NaNO_3$ as trace. Solid lines were obtained by SDEFM.

When $MgSO_4$ was used as trace salt, SO_4^{2-} and Mg^{2+} were highly rejected with rejections of 99% and around 85%, respectively at Jv around 40 µm/s. The rejection order obtained was $R(SO_4^{2-}) > R(Mg^{2+}) > R$ (NaCl). These patterns are in accordance with results reported in previous NF studies for NaCl [16–18], SO_4^{2-} [19,20] and Mg^{2+} [21] rejections.

Noteworthy is the rejection pattern of NO_3^- which shows much lower rejection and even negative values at low Jv. Negative rejections can be explained as reported in previous studies [14]. The magnitude of the electric field depends on the difference between the membrane permeability with respect to dominant salt ions, so that if the membrane permeability with respect to the dominant anion is smaller than to the dominant cation, there is a delay of the trace cation and an acceleration of the trace anion. On the other hand, if the membrane permeability with respect to the dominant cation permeability is lower than to the

anion, the trace anion is delayed and the trace cation is accelerated. Briefly, the electric field is capable to attract some ions, accelerating them and making their rejection values negative. Furthermore, the electric field is able to repulse trace ions, delaying them and making their rejections values higher.

3.2. $MgSO_4$ dominant

Fig. 3 shows the experimental rejections and the rejections predicted by the SDEFM with a solution of $MgSO_4$ as a dominant salt and NH_4Cl as trace for both configuration membranes.

Noticeable difference in the rejection patterns was observed with respect to the previous experiments. The dominant salt was highly rejected (almost 100%). The positive trace ion NH_4^+ was also fairly well rejected (around 80%).

As it was explained before, the trace rejection strongly depends on the dominant salt. Depending on the difference between the membrane permeabilities with respect to each dominant salt ion, the arisen electric field would be stronger or weaker. Comparing the current experiment (using magnesium as part of the dominant salt) with the first one showed (using magnesium as trace salt), the rejection of Mg^{2+} as trace ion depending on NaCl as dominant salt was lower. The reason of this behaviour lies in the fact that, using NaCl as dominant salt, the membrane permeability with respect to chloride is much higher than the membrane permeability with respect to sulphate when using $MgSO_4$ as dominant salt, so the arisen electric field in the case of NaCl is weaker and magnesium is less rejected than it is expected. On the other side, using $MgSO_4$ as dominant salt, the electric field strongly retards the cations making their rejections much higher than they are expected.

As before, the rejection pattern of the anion used as trace ion in the experiment, in this case Cl^-, showed much lower rejection and again negative values at low *Jv*. It can be stated that $R(MgSO_4) > R(NH_4) > R(Cl)$, which matches previous results reported in the literature [22]. For instance, Häyrynen et al. [23] calculated the retention for different ions, such as sulphate, magnesium and ammonium obtaining a rejection of 98.9, 81.8, and 56.2% for sulphate, magnesium, and ammonium, respectively.

It is important to point out that the membrane configuration does not appear to significantly affect the dominant salt or the trace ions rejections.

3.3. $MgCl_2$ dominant

Fig. 4 shows the experimental rejections and the rejections predicted by the SDEFM with a solution of $MgCl_2$ as a dominant salt and KCl as trace for both configuration membranes.

Using $MgCl_2$ as dominant salt, its rejection with both membrane configurations reported similar results. The monovalent cation rejection behaved similarly in both configurations. Moreover, the single charge trace cations rejection was always negative. In this case, the negative rejection for the trace cation was related to the membrane permeability with respect to magnesium is always much lower than with respect to the chloride. This fact leads trace cations to be accelerated with the electric field obtaining negative rejections. Thus, $R(MgCl_2) > R$ (monovalent cations) was the order obtained in this study.

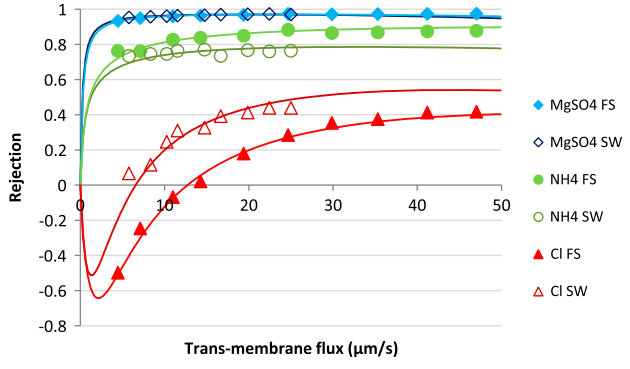

Fig. 3. Comparison between rejections experimentally obtained and rejections predicted with the SDEFM using a FS and a SW membrane configuration. $MgSO_4$ as dominant salt and NH_4Cl as trace. Solid lines were obtained by SDEFM.

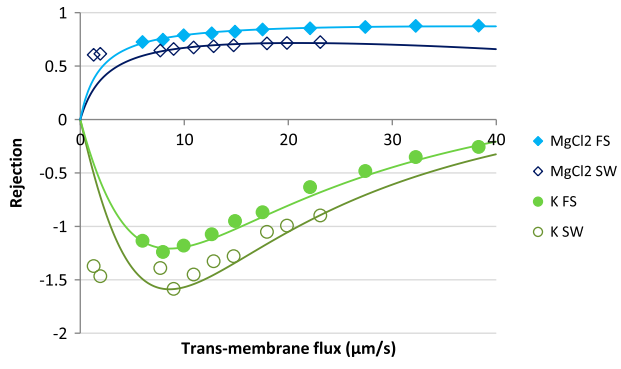

Fig. 4. Comparison between rejections experimentally obtained and rejections predicted with the SDEFM using a FS and a SW membrane configuration. $MgCl_2$ as dominant salt and KCl as trace. Solid lines were obtained by SDEFM.

As a general conclusion for all the experiments that were carried out, it can be stated that the *Jv* obtained in both membrane configurations were quite different. Working with a FS membrane configuration, higher values of *Jv* were obtained compared to those obtained using the SW configuration working at equal TMP with the same salt feed solution. This fact depends on the polarization layer thickness. At lower polarization layer thickness, higher *Jv* is obtained. Working at the same conditions, the thickness of the polarization layer was lower working with the FS configuration and, for this reason, the *Jv* obtained were higher.

3.4. Membrane permeability with respect to each ion

Results of membrane permeability with respect to each ion can be obtained by the SDEFM. Their order in each salt mixture allows understanding the electric effects for the ions rejection. Tables 3–5 summarize in decreasing order the membrane permeability with respect to each ion obtained for each one of the tests and also its value in both membrane configurations.

As can be seen in Table 3, three trace cases have been studied working with NaCl as a dominant salt in the solution: monovalent anions (I^-, Br^-, and NO_3^-), monovalent cations (NH_4^+ and K^+) and divalent trace ions (Mg^{2+} and SO_4^{2-}). When working with a single charge anion trace (NO_3^-), the membrane permeability with respect to sodium is the highest one, followed by the membrane permeability with respect to the trace anion and the lowest is reported for chlorine. By working with a monovalent trace cation (NH_4^+), the membrane permeability with respect to chloride is still the lowest one, although now the membrane permeability with respect to trace cation is as high as that to sodium. Finally, using a divalent salt as a trace ($MgSO_4$), the membrane permeability with respect to the double charge ions is much lower.

Table 3
Membrane permeability with respect to each ion for different salt mixtures in both membrane configurations using NaCl as dominant salt

Salt mixture (Dominant salt_Trace salt)	Membrane permeability with respect to each ion (μm/s)
NaCl_NaI	
NaCl_NaBr	
NaCl_$NaNO_3$	
NaCl_NH_4Cl	
NaCl_KCl	
NaCl_$MgSO_4$	

Table 4
Membrane permeability with respect to each ion for different salt mixtures in both membrane configurations using $MgSO_4$ or Na_2SO_4 as dominant salt

Salt mixture (Dominant salt_Trace salt)	Membrane permeability with respect to each ion (μm/s)
$MgSO_4$_NaI	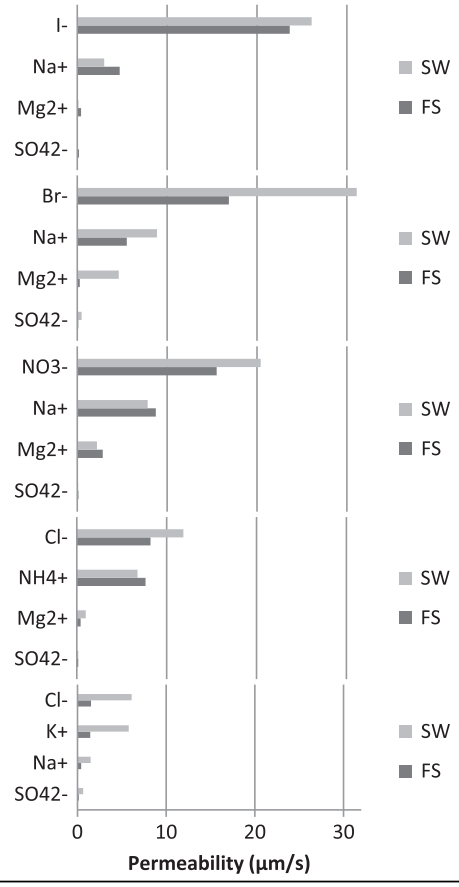
$MgSO_4$_NaBr	
$MgSO_4$_$NaNO_3$	
$MgSO_4$_NH_4Cl	
Na_2SO_4_KCl	

For $MgSO_4$ as dominant salt, two trace cases have been studied: trace monovalent anions (I^-, Br^-, and NO_3^-) and trace monovalent cation (NH_4^+ and K^+) (Table 4). In the former case, the membrane permeability with respect to the single charge anion is the highest one, followed by the membrane permeability with respect to sodium, magnesium and finally sulphate. In the case of KCl or NH_4Cl as salt traces, the membrane permeability order with respect to each ion is chloride, monovalent cation, magnesium and the lowest one sulphate again.

The same two trace cases have been studied using $MgCl_2$ as dominant salt (Table 5). The membrane permeability with respect to each ion was as follows: sodium > single charge anion > chloride > magnesium and monovalent cation > chloride > magnesium.

The results are consistent with previous studies [11,12,14,19], in which it was observed that the membrane NF270 exhibit less permeability to divalent ions. Besides, membrane permeability with respect to sulphate was lower than to magnesium, and the permeability to chloride was lower than the one obtained to sodium. According to Yaroshchuk et al. [15], the membrane permeability with respect to each ion of the dominant salt can explain the behaviour of the electric fields which controls the rejections of the trace ions during the experiments. And by means of Tables 3–5, it has been shown that they are fairly the same for both membrane configurations, being the permeability number of each ion in the same order of magnitude for each membrane configuration.

Table 5
Membrane permeability with respect to each ion for different salt mixtures in both membrane configurations using $MgCl_2$ as dominant salt

Salt mixture (Dominant salt_Trace salt)	Membrane permeability with respect to each ion (μm/s)
$MgCl_2$_NaI	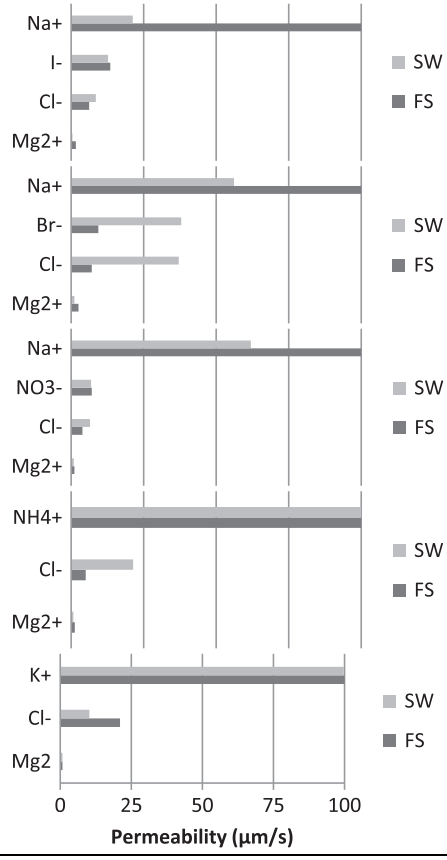
$MgCl_2$_NaBr	
$MgCl_2$_$NaNO_3$	
$MgCl_2$_NH_4Cl	
$MgCl_2$_KCl	

4. Conclusions

Comparing both membrane configurations, it can be said that the *Jv* obtained is higher using the FS membrane configuration working at the same pressure and salt mixture. The dominant salt rejection seems to be not affected by the membrane configuration, as similar rejection curves were obtained for both configurations. The general trend observed for the trace ion rejection was the same.

SDEFM is a valid model which is capable to fit satisfactorily experimental data of a dominant salt and a trace mixture and determinate the rejection curves for each of the ions vs. the *Jv* produced in each experiment. Moreover, according to the SDEFM, the rejection values obtained can be explained with the effect of the spontaneouslyarising electric fields.

Membrane permeability with respect to each ion can be calculated with the SDEFM, and for both membrane configurations, the permeability is similar. Furthermore, qualitatively, they have the same order of membrane permeability with respect to each ion, as it is shown in Tables 3–5.

In general terms, it seems that the two configurations behave in a similar way. This trend is useful implementing NF technology at industrial scale, since SW configuration is used at large scale, representing a larger membrane active area and occupying a small space, whereas the FS configuration is used in test in a laboratory scale, for its simplicity and its easiest methodology is of great interest in order to obtain experimental data.

Acknowledgments

This research was supported by the ZERO-DISCHARGE project (CTQ2011–26799) financed by "Ministerio de Economía y Competitividad" and the Catalan Government (Project Ref. 2014SGR050), Spain. The work of Mònica Reig was supported by the Spanish Ministry (MINECO) within the scope of the grant BES-2012–051914.

We want to thank the contribution of Dow Chemical for the supply of the membranes.

Glossary of symbols

A_{ef}	—	effective membrane area (m^2)
c_i	—	concentration of solute i (mol/m^3)
D_i	—	diffusion coefficient of the solute i (m^2/s)
f_s	—	reciprocal intrinsic transmission of the dominant salt
f_t	—	reciprocal intrinsic transmission of a trace
J_i	—	trans-membrane flux of the solute i (mol/m^2s)
Jv	—	trans-membrane flux (m/s)
m	—	liquid collected weight (kg)
$P_\pm$	—	membrane permeability to single ions of the dominant salt (m/s)
P_s	—	membrane permeability to the dominant salt (m/s)
P_t	—	membrane permeability to trace ions (m/s)
R_s^{int}	—	intrinsic rejection of the dominant salt
R_T^{int}	—	intrinsic rejection of the trace ion
tp	—	time of sample collection (s)
V	—	permeate volume collected during tp (m^3)
x	—	trans-membrane coordinate (m)
$Z_\pm$	—	charge to single ions of the dominant salt
z_i	—	solute i charge
Z_t	—	charge of the trace ion
σ	—	density at 25°C (kg/m^3)
φ	—	electrostatic potential

References

[1] M.I. Litter, M.E. Morgada, J. Bundschuh, Possible treatments for arsenic removal in Latin American waters for human consumption, Environ. Pollut. 158 (2010) 1105–1118.

[2] Y. Yoon, R. Lueptow, Removal of organic contaminants by RO and NF membranes. J. Membr. Sci. 261 (2005) 76–86.

[3] R.W. Baker, Membrane Technology and Applications, third ed., Wiley, Chichester, 2012.

[4] M. Pontié, C.K. Diawara, M. Rumeau, Streaming effect of single electrolyte mass transfer in nanofiltration: Potential application for the selective defluorination of brackish drinking waters, Desalination 151 (2003) 267–274.

[5] N. Hilal, H. Al-Zoubi, N.A. Darwish, A.W. Mohamma, M. Abu Arabi, A comprehensive review of nanofiltration membranes: Treatment, pretreatment, modelling, and atomic force microscopy, Desalination 170 (2004) 281–308.

[6] A.K. Pabby, S.S.H. Rizvi, A.M. Sastre, Handbook of Membrane Separations: Chemical, Pharmaceutical, Food, and Biotechnological Applications, Taylor & Francis group, CRC Press, Boca Raton, FL, 2009.

[7] L. Giorno, E. Drioli, Biocatalytic membrane reactors: Applications and perspectives, Trends Biotechnol. 18 (2000) 339–349.

[8] P. Hillis, Membrane Technology in Water and Wastewater Treatment, Royal Society of Chemistry, Cambridge, 2000.

[9] A.I. Schäfer, A.G. Fane, T.D. Waite, Nanofiltration: Principles and Applications, Elsevier Advanced Technology, Oxford, 2005.

[10] G. Ribera, L. Llenas, X. Martínez, M. Rovira, J. de Pablo, Comparison of nanofiltration membranes' performance in flat sheet and spiral wound configurations: A scale-up study, Desalin. Water Treat. 51 (2013) 458–468.

[11] A. Yaroshchuk, X. Martínez-Lladó, L. Llenas, M. Rovira, J. de Pablo, Solution-diffusion-film model for the description of pressure-driven trans-membrane transfer of electrolyte mixtures: One dominant salt and trace ions, J. Membr. Sci. 368 (2011) 192–201.

[12] A. Yaroshchuk, X. Martínez-Lladó, L. Llenas, M. Rovira, J. de Pablo, J. Flores, P. Rubio, Mechanisms of transfer of ionic solutes through composite polymer nanofiltration membranes in view of their high sulfate/chloride selectivities, Desalin. Water Treat. 6 (2009) 48–53.

[13] S. Pereira, K.-V. Peinemann, Membrane Technology: In the Chemical Industry, second ed., Wiley-VCH Verlag GmbH & Co. KGaA, Weinheim, 2006.

[14] N. Pages, A. Yaroshchuk, O. Gibert, J.L. Cortina, Rejection of trace ionic solutes in nanofiltration: Influence of aqueous phase composition, Chem. Eng. Sci. 104 (2013) 1107–1115.

[15] A. Yaroshchuk, M.L. Bruening, E.E. Licón Bernal, Solution-diffusion-electro-migration model and its uses for analysis of nanofiltration, pressure-retarded osmosis and forward osmosis in multi-ionic solutions, J. Membr. Sci. 447 (2013) 463–476.

[16] S. Lee, C. Lee, Effect of membrane properties and pretreatment on flux and NOM rejection in surface water nanofiltration, Sep. Purif. Technol. 56 (2007) 1–8.

[17] M. Pontié, H. Dach, J. Leparc, M. Hafsi, A. Lhassani, Novel approach combining physico-chemical characterizations and mass transfer modelling of nanofiltration and low pressure reverse osmosis membranes for brackish water desalination intensification, Desalination 221 (2008) 174–191.

[18] K. Walha, R.B. Amar, L. Firdaous, F. Quéméneur, P. Jaouen, Brackish groundwater treatment by nanofiltration, reverse osmosis and electrodialysis in Tunisia: Performance and cost comparison, Desalination 207 (2007) 95–106.

[19] M.-V. Galiana-Aleixandre, J.-A. Mendoza-Roca, A. Bes-Piá, Reducing sulfates concentration in the tannery effluent by applying pollution prevention techniques and nanofiltration, J. Clean. Prod. 19 (2011) 91–98.

[20] A. Bódalo, J.-L. Gómez, E. Gómez, G. León, M. Tejera, Reduction of sulphate content in aqueous solutions by reverse osmosis using cellulose acetate membranes, Desalination 162 (2004) 55–60.

[21] M.D. Afonso, J.O. Jaber, M.S. Mohsen, Brackish groundwater treatment by reverse osmosis in Jordan, Desalination 164 (2004) 157–171.

[22] H. Kurama, The application of membrane filtration for the removal of ammonium ions from potable water, Water Res. 36 (2002) 2905–2909.

[23] K. Häyrynen, E. Pongrácz, V. Väisänen, N. Pap, M. Mänttäri, J. Langwaldt, R.L. Keiski, Concentration of ammonium and nitrate from mine water by reverse osmosis and nanofiltration, Desalination 240 (2009) 280–289.